

CONTROL OF LASER RADIATION PARAMETERS

https://doi.org/10.1070/QEL18042

Attenuation of the intensities of spectral components of a multiwavelength pulsed laser system by means of the Bragg diffraction of radiation by several acoustic waves

A.S. Machikhin, M.O. Sharikova, A.I. Lyashenko, A.B. Kozlov, V.E. Pozhar, V.A. Lomonov, E. Stoikova

Abstract. **A method for controlling precisely the intensities of several spectral components of radiation generated by a multiwavelength laser system is described. The method is based on the use of simultaneous Bragg diffraction by a set of acoustic waves of corresponding frequencies and adjustment of their amplitudes. The efficiency of the proposed method is demonstrated by the example of a multiwavelength system based on a pulsed Nd:YAG laser (1064 nm) with intracavity parametric generation of a signal wave (1572 nm) and extracavity light conversion into higher harmonics and sum frequencies. An independent control of intensity ratio for four spectral components in the visible range (452, 532, 635, and 786 nm) is obtained by precisely controlled attenuation of acoustic-wave amplitudes using an original 4-channel acousto-optical polychromator.**

Keywords: *acousto-optics, Bragg diffraction, selective attenuation, pulsed Nd:YAG laser.*

1. Introduction

Multiwave methods of study are becoming more and more popular in practice, because spectral analysis in different ranges yields important information about an object in question, which are necessary to identify it and determine its composition, structure, and state. Lasers, which provide high brightness, narrow lines, and high spectral contrast, are especially promising as multiwavelength light sources. To obtain radiation at different wavelengths, methods of parametric generation and generation of harmonics, sum frequencies, and difference frequencies are applied.

Parametric generation of light, which is widely used in laser technologies and photonics [1, 2], is based on converting pump laser radiation in a nonlinear medium into idler and signal waves, whose sum frequency is equal to the pump frequency [3]. Optical parametric oscillators (OPOs) make it possible to convert laser radiation in a wide frequency range [4]. In particular, when several successive nonlinear conversions are used, a laser with an OPO provides simultaneous lasing at several desired frequencies [5, 6]. This approach is used in telecommunication systems [7], colour laser imaging devices [8], multispectral holography [9], and some other fields. In this case, the intensities of different spectral component may differ by 1 to 2 orders of magnitude.

To apply such multifrequency systems in practice, it is extremely important to be able to control the pulse power for each frequency and, in particular, equalise these powers. It is fairly difficult to equalise intensity components directly during lasing in view of the existing deterministic relationships between the components and different efficiencies of frequency conversion processes; therefore, one needs tools for precisely controlled attenuation of each component to a specified level.

Narrowband light filters that can be moved mechanically are suitable for continuous-wave systems, but pulsed systems call for more on-line control of all components simultaneously. In addition, using fixed-transmission filters, one cannot change gradually the component intensities. This can be done with the aid of classical electro-optical (EO) and acousto-optical (AO) modulators, but they are generally intended for controlling monochromatic light intensity [10]. Thus, the development of a method of nonmechanical controlled selective attenuation of polychromatic radiation of pulsed laser systems is an urgent task.

2. Method in proposal

Independent control of the intensity $I(\lambda_j)$ of different components of a multiwavelength laser system could be implemented by means of the Bragg diffraction of laser radiation by several acoustic waves with corresponding frequencies Ω_j in a photoelastic medium. This approach, using excitation of several independent ultrasonic waves in a medium, was applied previously to perform tunable rejection spectral filtering [11], solve problems in correlation spectroscopy [12], select several specified laser lines [13], equalise intensities in channels of fibre communication line [14], etc. To implement this approach, one must develop a specialised multifrequency AO cell and check the control efficiency and channel interference. Below we describe the principle of operation of a multifrequency spectral AO device, its composition, and structure.

When several spectral components undergo diffraction, each jth component should satisfy the Bragg phase-matching condition $\boldsymbol{k}_j^{\mathrm{i}} + \boldsymbol{q}_j = \boldsymbol{k}_j^{\mathrm{d}}$, which relates the wave vectors of the

A.S. Machikhin, M.O. Sharikova, A.I. Lyashenko, V.E. Pozhar Scientific and Technological Center of Unique Instrumentation, Russian Academy of Sciences, ul. Butlerova 15, 117342 Moscow, Russia; e-mail: sharikova.mo@ntcup.ru;
A.B. Kozlov JSC M.F. Stelmakh Polyus Research Institute, ul. Vvedenskogo 3, korp. 1, 117342 Moscow, Russia;
V.A. Lomonov Federal Scientific Research Centre 'Crystallography and Photonics', Russian Academy of Sciences, Leninsky prosp. 59, 119333 Moscow, Russia;
E. Stoikova Institute of Optical Materials and Technologies, Bulgarian Academy of Sciences, block 109, Acad. G. Bonchev str., 1113 Sofia, Bulgaria

Received 25 February 2022
Kvantovaya Elektronika **52** (5) 454–458 (2022)
Translated by Yu.P. Sin'kov

incident (i) and diffracted (d) light waves ($\boldsymbol{k}_j^{\mathrm{i,d}} = n^{\mathrm{i,d}}(\omega_j)\omega_j/c$) and the ultrasonic wave $\boldsymbol{q}_j = \Omega_j/V$. Here, ω_j and Ω_j are, respectively, the light and ultrasound frequencies; n^{i} and n^{d} are the refractive indices of anisotropic medium for the incident and diffracted beams, respectively; c is the speed of light in vacuum; and V is the speed of sound. Thus, the frequency of diffracted radiation is unambiguously related to the acoustic frequency determining the Bragg grating period. We used an AO cell based on a uniaxial TeO_2 crystal. In this cell, in the case of diffraction of extraordinary polarised wave in the $(1\bar{1}0)$ plane with a change in the polarisation direction (e → o), these frequencies are related as follows [10, 15]:

$$\Omega_j = \omega_j(V/c)\, n_{\mathrm{o}}(\omega_j) \times \left[\xi(\omega_j)\cos(\theta-\gamma) - \sqrt{1-\xi^2(\omega_j)\sin^2(\theta-\gamma)}\right], \qquad (1)$$

where, θ and γ are the propagation angles of the incident light and acoustic waves, respectively, relative to the [110] axis and $\xi(\theta) \equiv (n_{\mathrm{e}}(\theta))/n_{\mathrm{o}} = [\sin^2\theta + (n_{\mathrm{o}}/n_{\mathrm{e}})^2\cos^2\theta]^{-1/2}$ is the parameter characterising the degree of birefringence.

The light diffraction coefficient for the jth spectral component is related to the power density I_j^{ac} of applied acoustic field [10]:

$$\eta_j \equiv \frac{I_j^{\mathrm{d}}}{I_j^{\mathrm{i}}} = \sin^2\left(\pi\frac{L}{\lambda}\sqrt{\frac{M_2 I_j^{\mathrm{ac}}}{2}}\right), \qquad (2)$$

where $I_j^{\mathrm{i,d}}$ are the intensities of the incident and diffracted beams, L is the acousto-optic interaction length, $M_2 = n^6p^2/\rho V^3$ is the AO figure of merit, p is the effective photoelastic constant, and ρ is the density of the medium.

Thus, specifying [in correspondence with formulae (1) and (2)] a set of ultrasound frequency components Ω_j and varying their intensities I_j^{ac}, one can form a desired combination of AO filter transmission windows and perform precise control of radiation intensity at each jth wavelength in the range from 0 to 100%, i.e., ensure operation of AO crystal in the multichannel polychromator–attenuator mode. In practice, the maximum attainable diffraction coefficient is somewhat below 100% in view of the angular divergence of the light beam and some other factors. Using this approach, one can, for example, equalise the intensities of different spectral components (Fig. 1).

The device for controlling the radiation intensity is an AO polychromator with a function of varying the number of transmission windows, their position, and the transmittance in each of them. The device described here contains an AO cell based on a TeO_2 crystal with a cut angle $\gamma = 7°$. The acoustic emitter was a piezoelectric transducer based on a $LiNbO_3$ crystal, containing two sections 5×10 mm in size and matched in the ultrasound frequency range of 54–127 MHz, which, as follows from formula (1), corresponds to the spectral range of 450–900 nm. The front crystal face is oriented so as that, under normal incidence conditions, the light propagation angle in the crystal is close to optimal: $\theta = 73.85°$. For simultaneous excitation of four ultrasonic waves, the AO cell is equipped with a tunable direct digital frequency synthesiser (Analog Devices AD9959) with two dual-channel amplifiers (Fig. 2).

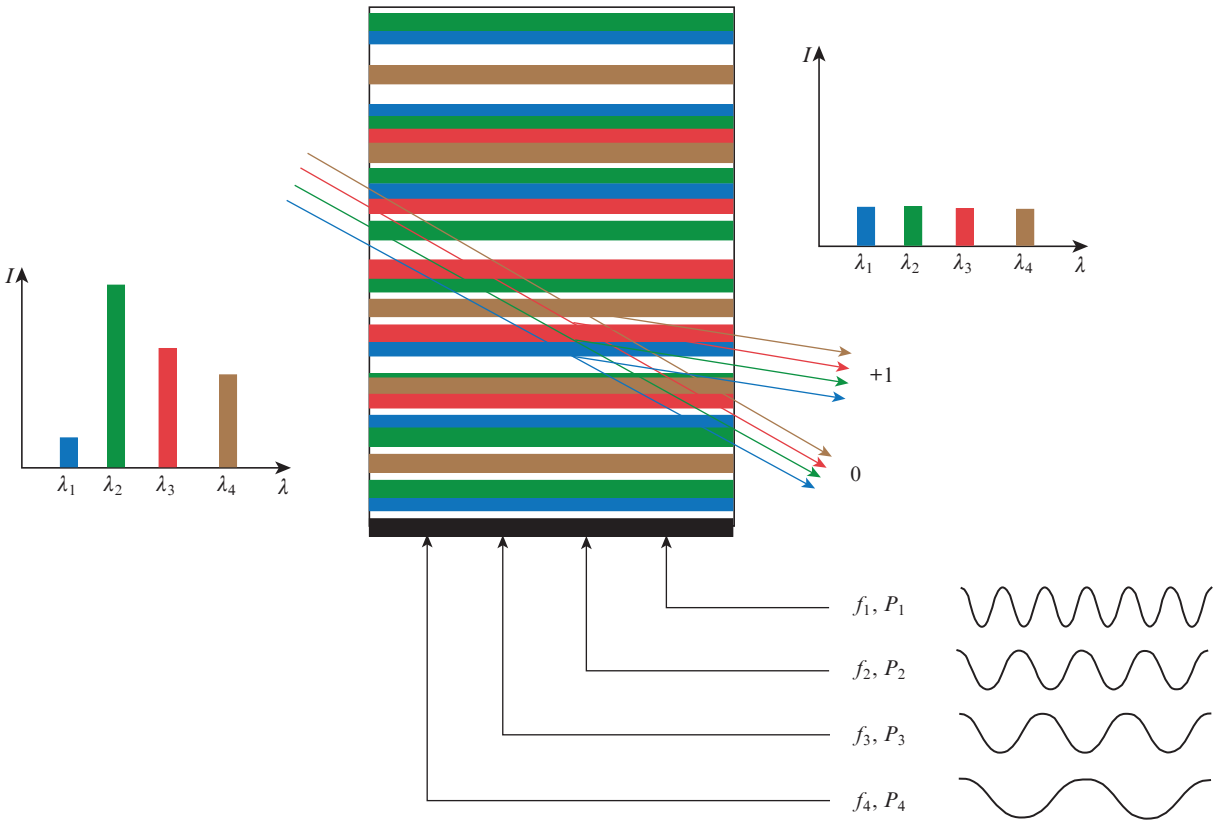

Figure 1. (Colour online) Bragg diffraction of polychromatic radiation by several acoustic waves with frequencies f_1–f_4 and powers P_1–P_4.

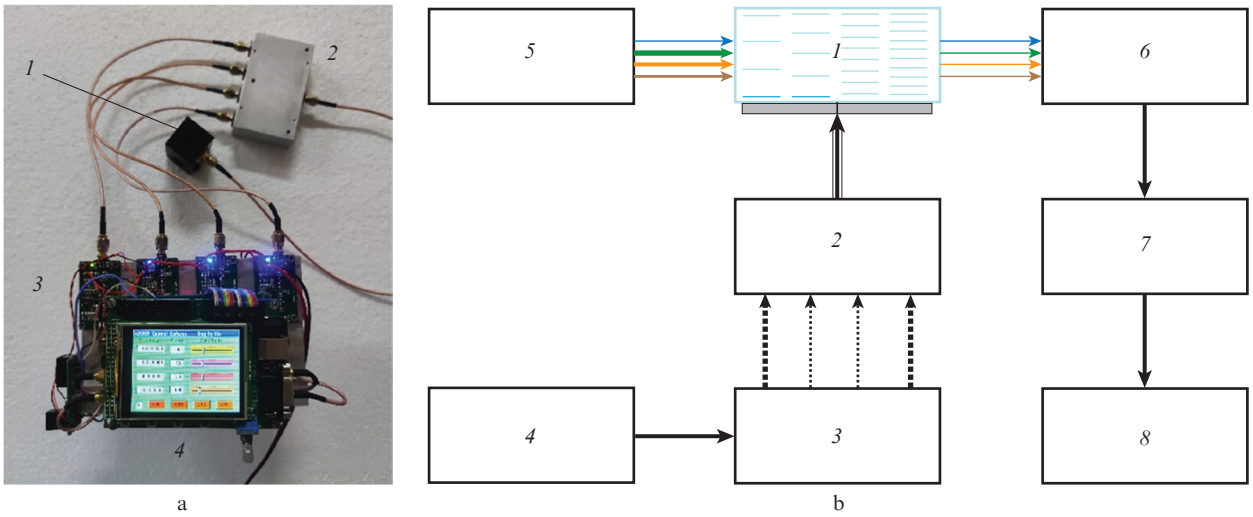

Figure 2. (Colour online) (a) Breadboard of a four-channel AO polychromator and (b) schematics of measurements on an experimental setup: (*1*) AO polychromator; (*2*) RF signal combiner; (*3*) RF synthesiser with two dual-channel amplifiers; (*4*) sensor screen; (*5*) multiwavelength laser system; (*6*) spectrometer; (*7*) computer; (*8*) monitor.

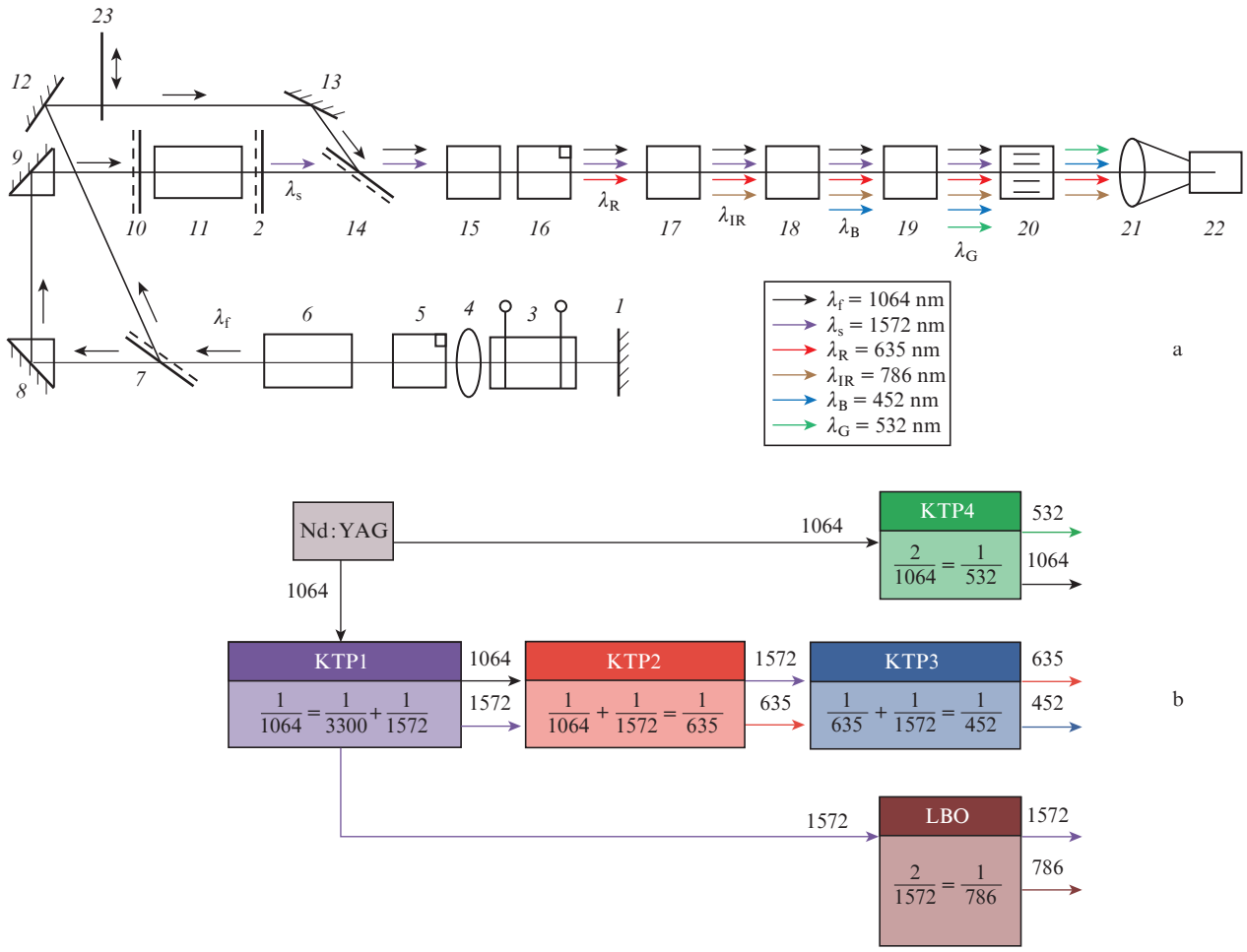

Figure 3. (Colour online) (a) Schematics of a multiwavelength laser system and (b) a diagram of frequency conversion for spectral components.

To test the proposed method, we designed an experimental setup based on a pulsed Nd:YAG laser (λ_f = 1064 nm) with intracavity parametric generation of a signal wave (λ_s =1572 nm) and extracavity conversion of radiation into higher harmonics and sum frequencies in nonlinear elements based on KTP and LBO crystals. The system provided simultaneous lasing at six wavelengths in the visible and near-IR ranges. The laser operated in the repetitively pulsed mode

(pulse repetition rate of 25 Hz, pulse duration of 200 μs, and pump pulse energy of 20 J). Specific frequencies of generated spectral components in this system can be changed. Their choice is determined by the problem to be solved.

The schematic of the multiwavelength laser system and the optical frequency conversion diagram are shown in Fig. 3. The laser cavity is formed by a highly reflecting mirror (*1*) and a selective mirror (*2*), which completely reflects radiation with λ_f and partially transmits radiation with λ_s. The radiation with λ_f is extracted using a polariser plate (*7*). A cylindrical active element (*6*), cut from a Nd:YAG crystal grown along the <100> direction, is azimuthally oriented so that the crystallographic axes *Y* and *Z* make angles of ±45° with the transmission plane of the polariser (*7*). Between an electro-optical element (*3*) [DKDP (KD_2PO_4) crystal] and the active element (*6*), there is a positive lens (*4*) and a rotator (*5*) of the plane of polarisation of light by 90°, which is made of optically active crystalline quartz; this rotator provides partial mutual compensation of induced birefringence in the active and electro-optical elements. The OPO cavity based on a nonlinear element (*11*) [KTP1 crystal ($\theta = 90°$, $\varphi = 0°$)] is formed by mirror *2* and selective mirror *10*, which completely reflects radiation at λ_s and is maximally transparent for radiation with λ_f. Between the polariser (*7*) and selective mirror *10*, there are two rotational prisms (*8*) and (*9*). The location of the electro-optical element (*3*) and the polariser (*7*) in the cavity at different sides from the active element (*6*) made it possible to implement three different operation modes of this device: generation of radiation with λ_f, generation of eye-safe radiation with λ_s, and simultaneous generation of radiations with λ_f and λ_s. The emerging laser beams with wavelengths λ_s and λ_f are converged using mirrors *12*, *13*, and a selective mirror (*14*), which reflects radiation with λ_f and transmits radiation with λ_s. A mobile screen (*23*) makes it possible to close the channel for the pump wave with λ_f and select radiation with the second-harmonic wavelength ($\lambda_{IR} = \lambda_s/2 = 786$ nm) in nonlinear element *17* [LBO ($\theta = 20.9°$, $\varphi = 90°$)] and residual radiation with λ_s. Radiation at the sum frequency, $1/\lambda_R = 1/\lambda_f + 1/\lambda_s$, which falls in the red spectral region ($\lambda_R = 635$ nm), is generated in the output laser cascade in a nonlinear optical element (*15*) [KTP2 crystal ($\theta = 53°$, $\varphi = 0°$)], after which a 90° rotator (*16*) of the plane of polarisation of radiation with λ_f is installed. Radiation at another sum frequency, $1/\lambda_B = 1/\lambda_s + 1/\lambda_R$, which falls in the blue spectral region ($\lambda_B = 452$ nm), is generated in the next element *18* [KTP3 crystal ($\theta = 70°$, $\varphi = 0°$)]. Residual radiation with a wavelength λ_f is converted in element *19* [KTP4 crystal ($\theta = 90°$, $\varphi = 23°$)] into the second harmonic, which falls in the green spectral region ($\lambda_G = \lambda_f/2 = 532$ nm).

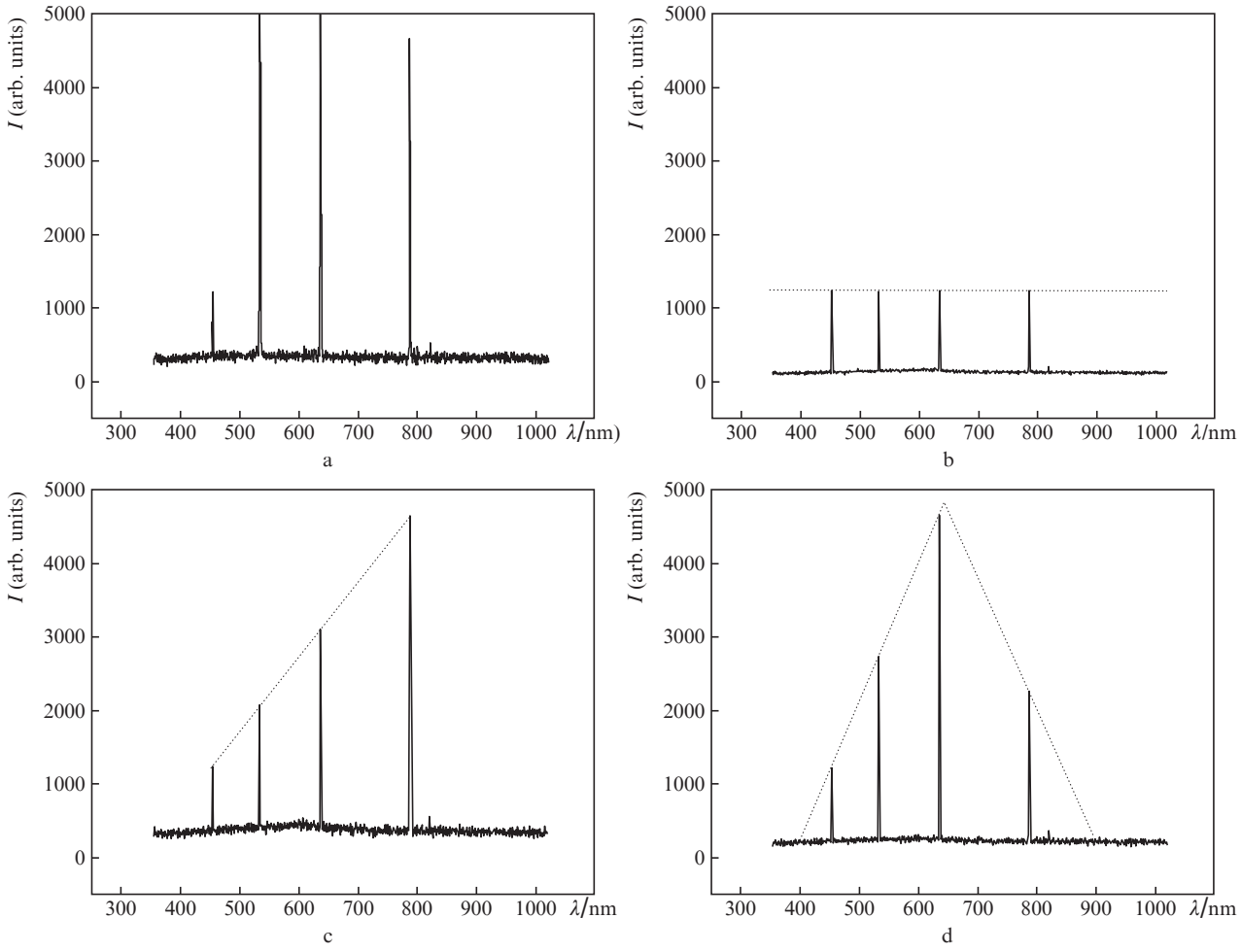

Figure 4. Laser radiation intensity (a) prior to and (b–d) after the AO attenuation in the modes of (b) equalisation of amplitudes, (c) their linear rise, and (d) apodisation by a triangular function. For convenience of comparison, all plots are shown of the same scale in arbitrary units [in Fig. 4a, the intensities of spectral components at wavelengths of 532 and 635 nm significantly go beyond the selected scale].

Table 1.

λ_j/nm	Light filters	Average power/mW	Pulse energy/mJ	Pulse duration/ns
$\lambda_B = 451.6$	SS-4 + SZS-22	0.2	0.008	5
$\lambda_G = 531.5$	SZS-22	4.6	0.186	7
$\lambda_R = 634.9$	SZS-24 + OS-14	3	0.12	5
$\lambda_{IR} = 786.4$	FS-7	2.2	0.088	5

Thus, simultaneous stable pulsed lasing with a repetition rate of 25 Hz at six wavelengths is implemented; four of these wavelengths (λ_G, λ_B, λ_R, and λ_{IR}) fall in the matching range of the developed four-channel AO polychromator attenuator (*20*). The energy parameters of pulses of these harmonics, polarised linearly in the horizontal plane, were measured when selecting each spectral component using light filters; these parameters are listed in Table 1. The pulse widths at half maximum were measured using an avalanche photodiode (LFD-2) and an oscilloscope (LeCroy WaveRunner 8254R). It can be seen form Table 1 that the pulse energies for different spectral components differ by more than an order of magnitude, a circumstance hindering their simultaneous efficient use.

The polychromator attenuator (*20*) is installed at the output of the laser system; it is tuned to frequencies f = 126.5, 100.3, 84, and 63.4 MHz, which correspond to the transmission peaks at the wavelengths λ_B, λ_G, λ_R, and λ_{IR}. The light transmitted through the attenuator is directed by an objective (*21*) to the input window of a diffraction spectrometer (*22*) (Ocean Optics FLAME-CHEM-VIS-NIR).

The emission spectra of the laser system without AO attenuation (at applied acoustic powers $P_B = 0.3$ W, $P_G = 0.2$ W, $P_R = 0.26$ W, and $P_{IR} = 0.2$ W) are presented in Fig. 4a. Figure 4b shows the same spectra recorded with AO filter operating in the mode of equalisation of laser line intensity at the level I_B of the weakest blue component and applied powers $P_B = 0.3$ W, $P_G = 0.17 \times 10^{-3}$ W, $P_R = 0.06$ W, and $P_{IR} = 0.09$ W. Figure 4c presents the spectra measured with a linear increase in intensities from the level I_B (for the shortest wavelength component) to the level I_{IR} of the longest wavelength component, which is implemented at $P_B = 0.3$ W, $P_G = 0.25 \times 10^{-3}$ W, $P_R = 0.1$ W, and $P_{IR} = 0.2$ W. The spectra recorded with component intensities adjusted to a specified envelope in the form of a triangle ($P_B = 0.3$ W, $P_G = 0.5 \times 10^{-3}$ W, $P_R = 0.13$ W, $P_{IR} = 0.12$ W) are shown in Fig. 4d.

3. Conclusions

The Bragg diffraction of radiation by several acoustic waves makes it possible to control precisely and in wide ranges the amplitudes of individual spectral components of a multiwavelength pulsed laser system. Setting a certain component intensity ratio, one can compensate for the influence of the spectral properties of the medium through which radiation propagates, the spectral dependence of photodetector sensitivity, and many other factors.

The possibility of implementing this method was demonstrated by the example of controlling amplitudes of four spectral components of a multiwavelength laser system; however, it can also be applied in systems with a much larger number of spectral channels. The attainable spectral range is not limited by only the visible region; it is determined by the operating range of the AO cell, which generally does not exceed one octave ($\lambda_{max}/\lambda_{min} \approx 2$) in the transparency window of the AO crystal. The above-described method of precise intensity control can be used to solve many practical problems related to simultaneous detection and processing of radiation at different wavelengths: in telecommunication, multispectral visualisation, multiplexed digital holography, etc.

Acknowledgements. This work was supported by the Russian Foundation for Basic Research (Project No. 20-58-18007) using equipment of the Center for Collective Use of the Scientific and Technological Centre of Unique Instrumentation of the Russian Academy of Sciences. The work in the part concerning fabrication of AO crystals was performed within the State Task for the Federal Scientific Research Centre 'Crystallography and Photonics' of the Russian Academy of Sciences.

References

1. Orr B.J., Haub J.G., White R.T. *Spectroscopic Applications of Pulsed Tunable Optical Parametric Oscillators, Tunable Laser Applications* (New York: CRC Press, 2016).
2. Lawrie L.A.W., Golding P.S., King T.A. *Proc. SPIE*, **2676**, Biomedical Sensing, Imaging, and Tracking Technologies I (24 April 1996). DOI: 10.1117/12.238821.
3. Akhmanov S.A., Khokhlov R.V. *Zh. Eksp. Teor. Fiz.*, **43**, 351 (1962).
4. Kolker D.B., Kostyukova N.Y., Boyko A.A., Badikov V.V., Badikov D.V., Shadrintseva A.G., Tretyakova N.N., Zenov K.G., Karapuzikov A.A., Zondy J.J. *J. Phys. Communications*, **2**, 035039 (2018).
5. Wallenstein R. Patent US5828424A (1998).
6. Paschotta R., Sudmeyer T., Weingarten K., Hanna D.C. Patent US7016103B2 (2006).
7. Lu X., Moille G., Singh A., Qing Li, Westly D.A., Rao A., Yu S.-P., Briles T.C., Papp S.B., Srinivasan K. *Optica*, **6**, 1535 (2019).
8. Snell K.J., Lee D., Pati B., Moulton P.F. *Proc. SPIE*, **3954**, *Projection Displays 2000: Sixth in a Series* (25 April 2000). DOI: 10.1117/12.383366.
9. Machikhin A., Polschikova O., Vlasova A., Lyashenko A., Dmitriev I., Batshev V., Bulatov M., Pozhar V. *Opt. Lett.*, **44**, 5025 (2019).
10. Yariv A., Yeh P. *Optical Waves in Crystals: Propagation and Control of Laser Radiation* (New York: Wiley, 1984; Moscow: Mir, 1987).
11. Suhre D.R., Theodore J.G. *Appl. Opt.*, **35**, 4494 (1996).
12. Mazur M.M., Suddenok Yu.A., Pozhar V.E. *Zh. Tekh. Fiz.*, **128**, 284 (2020).
13. Desse J., Picart P., Tankam P. *Opt. Express*, **16** (8), 5471 (2008).
14. Kastelik J.-C., Yushkov K., Dupont S., Voloshinov V. *Opt. Express*, **17** (15), 12767 (2009).
15. Pozhar V., Machihin A. *Appl. Opt.*, **51**, 4513 (2012).